Monthly Notices
of the
ROYAL ASTRONOMICAL SOCIETY

MNRAS **466,** 884–891 (2017)
Advance Access publication 2016 November 30

doi:10.1093/mnras/stw3109

# Search for Type Ia supernova NUV–optical subclasses

David Cinabro,[1]★ Daniel Scolnic,[2]† Richard Kessler,[2,3] Ashley Li[2] and Jake Miller[1]

[1]*Department of Physics and Astronomy, Wayne State University, Deroit, MI 48202, USA*
[2]*Kavli Institute for Cosmological Physics, University of Chicago, Chicago, IL 60637, USA*
[3]*Department of Astronomy and Astrophysics, University of Chicago, Chicago, IL 60637, USA*

Accepted 2016 November 28. Received 2016 November 9; in original form 2016 August 29

**ABSTRACT**

In response to a recently reported observation of evidence for two classes of Type Ia supernovae (SNe Ia) distinguished by their brightness in the rest-frame near-ultraviolet (NUV), we search for the phenomenon in publicly available light-curve data. We use the SNANA supernova analysis package to simulate SN Ia light curves in the Sloan Digital Sky Survey (SDSS) Supernova Search and the Supernova Legacy Survey (SNLS) with a model of two distinct ultraviolet classes of SNe Ia and a conventional model with a single broad distribution of SN-Ia ultraviolet brightnesses. We compare simulated distributions of rest-frame colours with these two models to those observed in 158 SNe Ia in the SDSS and SNLS data. The SNLS sample of 99 SNe Ia is in clearly better agreement with a model with one class of SN Ia light curves and shows no evidence for distinct NUV sub-classes. The SDSS sample of 59 SNe Ia with poorer colour resolution does not distinguish between the two models.

**Key words:** supernovae: general.

## 1 INTRODUCTION

A recent claim in Milne et al. (2015) is that there are two distinct groups of Type Ia Supernovae (SNe Ia) distinguished by their brightness in rest-frame near-ultraviolet (NUV). The light curves of the two sets, red and blue, differ by 0.46 mag in their $u - v$ colours at the time of peak brightness in the rest-frame $B$ band ($B$-peak) where the colour is derived from spectrophotometry of 23 SNe Ia observed with the UVOT instrument on the *Swift* satellite (Roming et al. 2005) and 52 SNe Ia observed with Keck and the Very Large Telescope with spectrophotometry matched to the UVOT system. The two sets have a 0.34 mag difference in the $u - b$ colour and an insignificant difference in the $b - v$ colour at peak brightness. Further, the fractions of SN Ia in the red and blue sets change as a function of redshift with the red sample dominant (60–70 per cent of the total) at redshifts smaller than 0.1, and the blue sample dominant (80–90 per cent of the total) at redshifts from 0.4 to 1.0. The study also found that SNe Ia in the red sample exhibited larger ejecta velocities in their spectral features. Milne et al. (2015) claim that SNe Ia light-curve fits for the red sample will underestimate the host galaxy extinction, leading to a redshift-dependent bias in the corrected peak brightness and also in the inferred cosmological parameters.

The importance of SNe Ia in modern cosmology cannot be understated. Observations just before the turn of the century provided the first clear evidence of an accelerated expansion of the Universe (Riess et al. 1998; Perlmutter et al. 1999) and subsequent observations combined with the clustering of galaxies and the cosmic microwave background point towards this acceleration being caused by a negative pressure fluid, dubbed dark energy (Olive & Particle Data Group 2014). These observations and the precision of the extraction of cosmological parameters inferred from SNe Ia depend on the assumption that the light curves of SNe Ia at low redshift are standardized in the same way as SNe Ia at high redshift. The observations of Milne et al. (2015) call this underpinning assumption into question.

The modelling of the rest-frame ultraviolet brightnesses of SNe Ia is more difficult than in the visible. SNe Ia are dimmer in the rest-frame ultraviolet than the visible, the effects of extinction are larger in the ultraviolet, and ground-based observations are difficult with large and highly variable ultraviolet atmospheric absorption. The joint light-curve analysis (JLA; Betoule et al. 2014) is the largest sample to date used for SN Ia cosmology, and they have publicly released many high-quality SN Ia light curves. In the JLA, the ultraviolet behaviour of SN Ia is empirically modelled with a distribution of brightnesses that is much broader than the distribution in the visible. This model does not agree with the Milne et al. (2015) observation of two narrow and distinct distributions in the ultraviolet.

Checking the claim of Milne et al. (2015) with the JLA data is not as simple as it might seem. At low redshift, the JLA sample is made of a heterogeneous collection of SN Ia light curves observed by many different instruments and surveys. Unknown selection effects for this sub-sample make it difficult to interpret (Scolnic et al. 2014).

★ E-mail: david.cinabro@wayne.edu
† Hubble, KICP Fellow.

**Table 1.** Central wavelengths of the filters used in this work. Details of the UVOT filters can be found in Breeveld et al. (2011) and for the SDSS and SNLS filters in Betoule et al. (2014). The UVOT filters are similar to the standard Bessel filters.

| Name | Central wavelength (Å) |
|---|---|
| UVOT-*u* | 3465 |
| UVOT-*b* | 4392 |
| UVOT-*v* | 5468 |
| SDSS/SNLS-*g* | 4760 |
| SDSS/SNLS-*r* | 6230 |
| SDSS/SNLS-*i* | 7630 |
| SDSS/SNLS-*z* | 9130 |

To avoid possible biases from selection effects, we use the SDSS-II (Frieman et al. 2008) and Supernova Legacy Survey (SNLS) (Astier et al. 2006) SN Ia samples, whose selection effects are well modelled with Monte Carlo simulations (Kessler et al. 2013; Betoule et al. 2014). However, these samples are not well suited to ultraviolet photometry. The Sloan Digital Sky Survey (SDSS) *u* filter is less efficient than the *g*, *r*, *i* filters, and the survey found only 12 securely identified SNe Ia at a redshift smaller than 0.1, which could be used to directly check the Milne et al. (2015) observation. The SNLS data do not provide ultraviolet filter photometry. With insufficient ultraviolet SN Ia data in the public domain, a more promising approach is to look at a higher redshift where the rest-frame ultraviolet is observed in the visible. From redshift of 0.3–0.7, the spectral range of the rest-frame UVOT *u*, *v* and *b* filters is observed in the SDSS and SNLS *g*, *r* and *i* filters.

The next section describes the models of SN Ia light curves that we used to check the observations in Milne et al. (2015). Section 3 describes our simulations of the SDSS-II and SNLS surveys, and the predictions based on our model of the Milne et al. (2015) observation. In Section 4, we compare the observed SN Ia light curves with the two models, and we end with a short conclusion.

## 2 SN Ia MODELS

We use the publicly available SNANA (Kessler et al. 2009)[1] package to perform the analysis described below. SNANA is a supernova light-curve analysis package that allows for detailed simulations of SN Ia light curves for arbitrary instruments, cadences and observing conditions. To develop a model for the Milne et al. (2015) observations, we simulate SN Ia light curves with infinite photon statistics observed with an error-free instrument at redshift of 0.01, called 'perfect mode', to view and compare rest-frame models without instrumental effects. We observe the time dependence of the colours and *B*-peak colours in the filters on the UVOT instrument (Breeveld et al. 2011). Our goal here is to develop an SN Ia light-curve model that reproduces the Milne observations and compare it to an existing, more conventional description of SNe Ia ultraviolet brightness.

We simulate light curves in the UVOT passbands to compare with Milne et al. (2015), and also in the SDSS and SNLS passbands, as described in the JLA (Betoule et al. 2014), to compare with data. The filters of the SDSS and SNLS are similar, but not exactly the same. Table 1 gives the central wavelengths of the filters that we reference in this work.

[1] http://snana.uchicago.edu

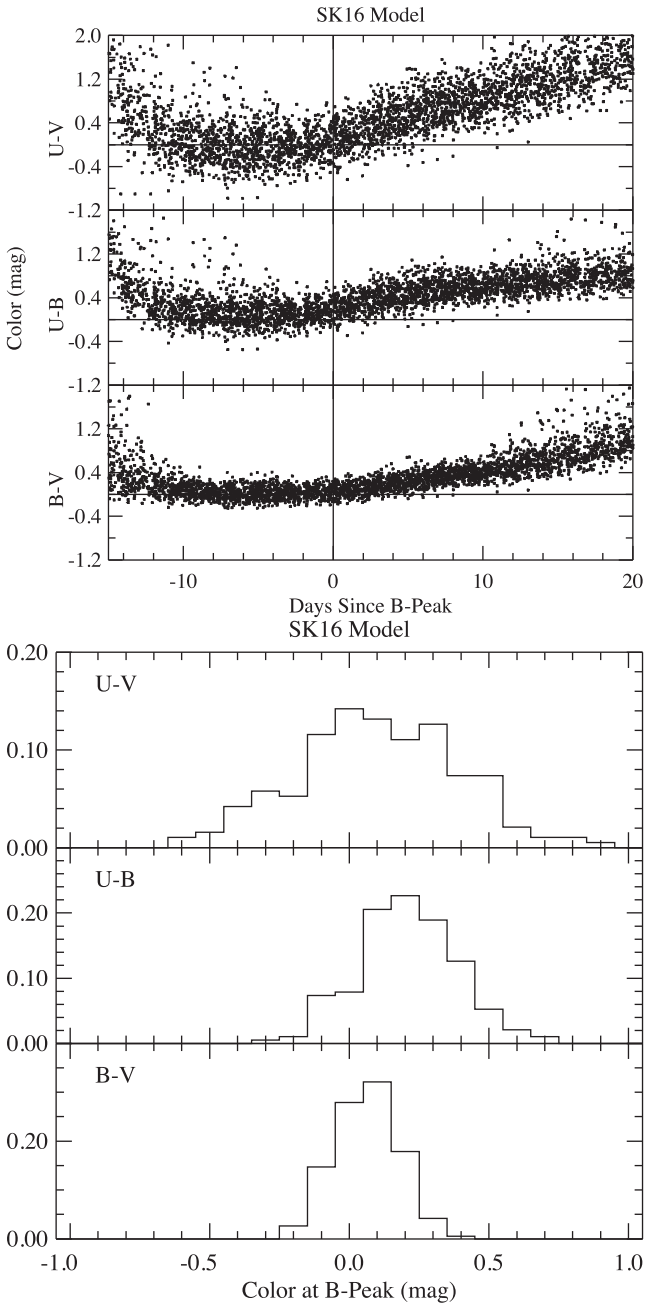


**Figure 1.** Rest-frame colours in the UVOT filters for the SK16 model in SNANA perfect mode as described in the text of SN Ia versus the time since the *B*-peak (top panel) and within one day of the *B*-peak (bottom panel).

Our base model for SN Ia light curves is the SALT-II model (Guy et al. 2010). The model describes the shape of light curves with two parameters, $x_1$, which gives the width–luminosity relation, and $c$, the colour parameter, which parametrizes intrinsic SN Ia colours and the effect of extinction. The parent population of these parameters used in our conventional simulation follow those measured by Scolnic & Kessler (2016), and thus we call this the SK16 model. Fig. 1 shows the time dependence of the rest-frame colours in the UVOT filters and within one day of *B*-peak in this SK16 model. The model includes the effect of Milky Way extinction from Schlegel, Finkbeiner & Davis (1998). The observed scatter is due to a combination of intrinsic brightness variations, the underlying population of colour ($c$) and stretch ($x_1$) and Milky Way extinction. In this

model, the ultraviolet part of the spectrum shows a larger scatter than in the visible.

We develop a model of the Milne et al. (2015) observation by introducing two classes of light curves distinguished by their brightnesses in the ultraviolet part of the spectrum. The resolution of the UVOT photometry, the red and blue histograms in fig. 2 of Milne et al. (2015) showing the $u - v$ colour for example, is between 0.05 and 0.07 mag (Milne, private communication). Given the observed width of the two-colour peaks, in the range of 0.07–0.09 mag, this implies that the contribution to the width due to the properties of the observed SN Ia (the stretch distribution and Milky Way extinction) is very narrow, less than 0.05 mag.

To reproduce the observed features, we modify the base prediction of the SALT-II rest-frame spectral flux, $F$, in the wavelength range 2700–4300 Å by

$$F = F^{(-0.4\ \mathrm{dm})}, \tag{1}$$

where

$$\mathrm{dm} = \pm\left(\frac{0.55}{2}\right)\sin\left(\pi\frac{(\lambda - 2700\ \text{Å})}{1600\ \text{Å}}\right)(1 + 0.04R_{\mathrm{G}})\ \mathrm{mag}. \tag{2}$$

The wavelength, $\lambda$, is in Angstroms and $R_{\mathrm{G}}$ is a Gaussian distributed random number with a standard deviation of 1. The amplitude and wavelength range of this bifurcation is chosen to match the colour separations in Milne et al. (2015). The amplitude is larger than the observed $u - v$ colour separation as it represents the maximum separation at only one wavelength, while the colour comes from integrating over the wavelength range of the $u$ filter. The size of the Gaussian smearing reproduces the narrow width of the NUV peaks. Over the entire wavelength range, there is an additional coherent scatter drawn from a Gaussian with a width of 0.08 mag matching the width of the SNe Ia brightness distribution. Those light curves with the brighter ultraviolet distortion are the 'blue' sample and those with the dimmer are the 'red' sample, and a random selection between the two is made for each light curve.

We find that equations (1) and (2) combined with non-zero values for the SALT-II $c$ parameter result in $u - v$ colour peaks that are too broad to be consistent with the Milne et al. (2015) observation. To preserve the sharp colour features, we set the SALT-II colour parameter, $c$, to zero. With $c = 0$, Fig. 2 shows time dependence of the rest-frame colours in the UVOT filters and the colours within one day of $B$-peak in this 'Milne-like' model. At $B$-peak, the width and separation of the red and blue peaks in the $u - v$ and $u - b$ colours agree well with Milne et al. (2015). The population of the two classes is equal in these illustrations. This model reproduces well the data displayed in figs 1–3, 9–12 and table 2 in Milne et al. (2015). It also incorporates the same variations of the SALT-II $x_1$ parameter and expected Milky Way extinction as we use in the SK16 model described above.

In the Milne-like model, variation in an extracted value of the SALT-II colour parameter away from zero is caused by the two different classes of SNe Ia in the ultraviolet, red and blue, rather than an underlying intrinsic colour population as described in Scolnic & Kessler (2016). Other choices for the parameters of the bifurcation given in equation (2) such as narrowing the wavelength range to 2700–3700 Å or reducing the magnitude of the separation are discussed further in Section 4.

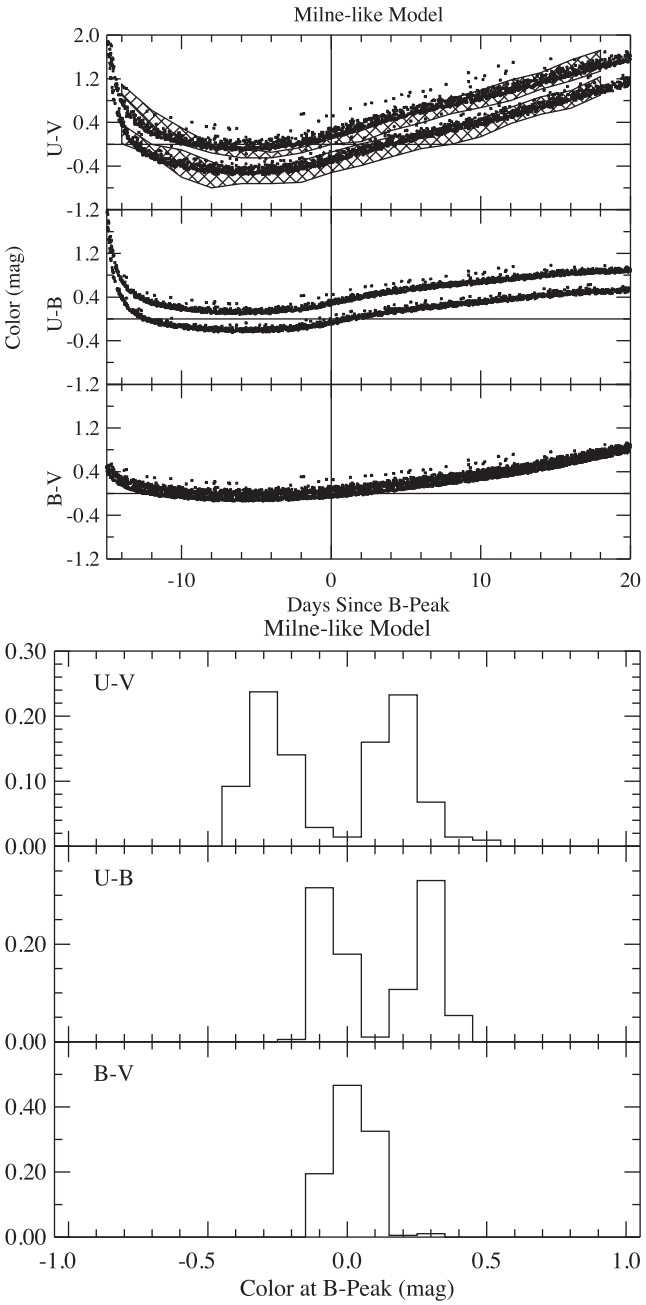


**Figure 2.** Using the SNANA 'perfect mode' simulation for the Milne-like model, the top panel shows UVOT rest-frame colours versus time and the bottom panel shows rest-frame colours within one day of $B$-peak. In the topmost panel, showing the $u - v$ colour versus time, the hatched regions are the range of red, upper, and blue, lower, sample colours taken from fig. 1 of Milne et al. (2015).

## 3 SIMULATION OF SN Ia SURVEYS

Using the SK16 and Milne-like models, we simulate SN Ia light curves corresponding to the SDSS and SNLS data in the JLA. Our goal here is to use the JLA data to compare against the two models when all observational effects are included, and develop a method of choosing between the two models. The simulations of the SDSS and SNLS supernova surveys include the exact cadence of observations, photometric uncertainties, redshift distributions and spectroscopic identification efficiencies observed in the surveys.

To ensure robust light-curve fits, we apply selection requirements to both the data and simulation. We require at least five epochs of observation in at least three of the $g$, $r$, $i$ and $z$ bands. Observations

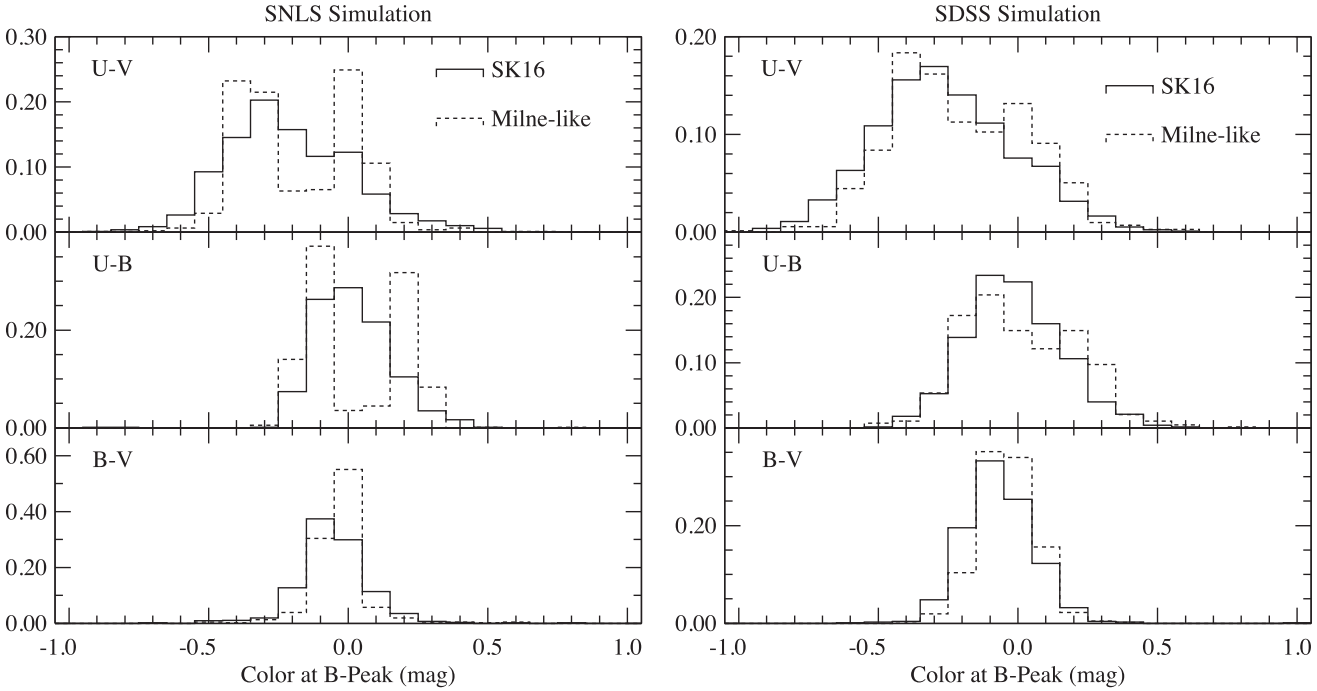


**Figure 3.** The fitted values of the rest-frame colours at *B*-peak for the SK16 and Milne-like models as described in the text for simulations of the SNLS (left-hand panel) and SDSS (right-hand panel) surveys.

must have a flux measured with signal to noise better than 3.0 in $g$, $r$, $i$ and 1.0 in $z$. Light curves passing these criteria are fit with the SALT-II model. We only consider epochs within −15 and +50 d of the fitted *B*-peak in the rest frame. The results of the fit are accepted if there is at least one epoch before and three after the *B*-peak, and the fit has a $\chi^2$ probability of greater than 0.001. We simulate samples that are about 15 times larger than the data samples. We consider SN Ia with redshifts in the range 0.3–0.4 for the SDSS and 0.3–0.7 for the SNLS.

These selections mirror the requirements on the JLA sample except that we require the presence of $z$-band photometry. The simulation predicts that 9 per cent of SNe Ia light curves in the JLA sample in the indicated redshift ranges will not pass to our sample.

We extract the rest-frame colours using the fitting procedure described in section 4.3 of Kessler et al. (2013). Briefly, after an initial fit to the SALT-II model, additional constrained fits are done to the photometry results of the two observer frame filters that most closely correspond to the best match in redshifted wavelength to the desired rest-frame filter photometry. The procedure introduces a negligible additional uncertainty on the rest-frame colours, and allows direct comparisons between the photometric observations of SDSS and SNLS with the spectrophotometric observations in Milne et al. (2015). Fig. 3 shows the distribution of colours at *B*-peak we expect from the two surveys for the two models.

The analysis of simulated SNe Ia shows that we could clearly distinguish between the Milne-like model, with two peaks clearly seen in the distribution of the $u - v$ colour, and the SK16 model, with the $u - v$ colour distribution appearing as one broad peak, in the SNLS survey. In the SDSS survey, it is more difficult to see a difference with only a hint of two peaks for the Milne-like model, but the SK16 model produces a slightly narrower distribution of the $u - v$ and $u - b$ colours than the SK16 model. The resolution of the *B*-peak colours of the SNLS is better than the SDSS.

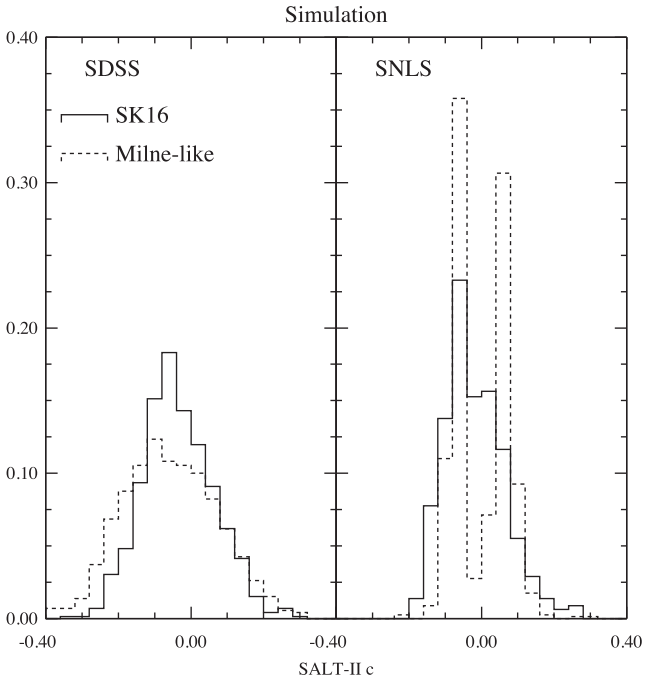


**Figure 4.** For simulations of the SK16 (solid lines) and Milne-like (dashed lines) models, the fitted SALT-II colour parameter ($c$) is shown for SDSS (left-hand side) and SNLS (right-hand side).

Further, we note that the fitted SALT-II colour parameter is also sensitive to the two models. Fig. 4 shows the distribution of the fitted value for $c$ in the two simulated surveys for the two models. There is a clear difference between the two models. The SNLS simulation shows two narrow peaks for the Milne-like model and one broad peak for the SK16 model. The simulation of the SDSS shows a

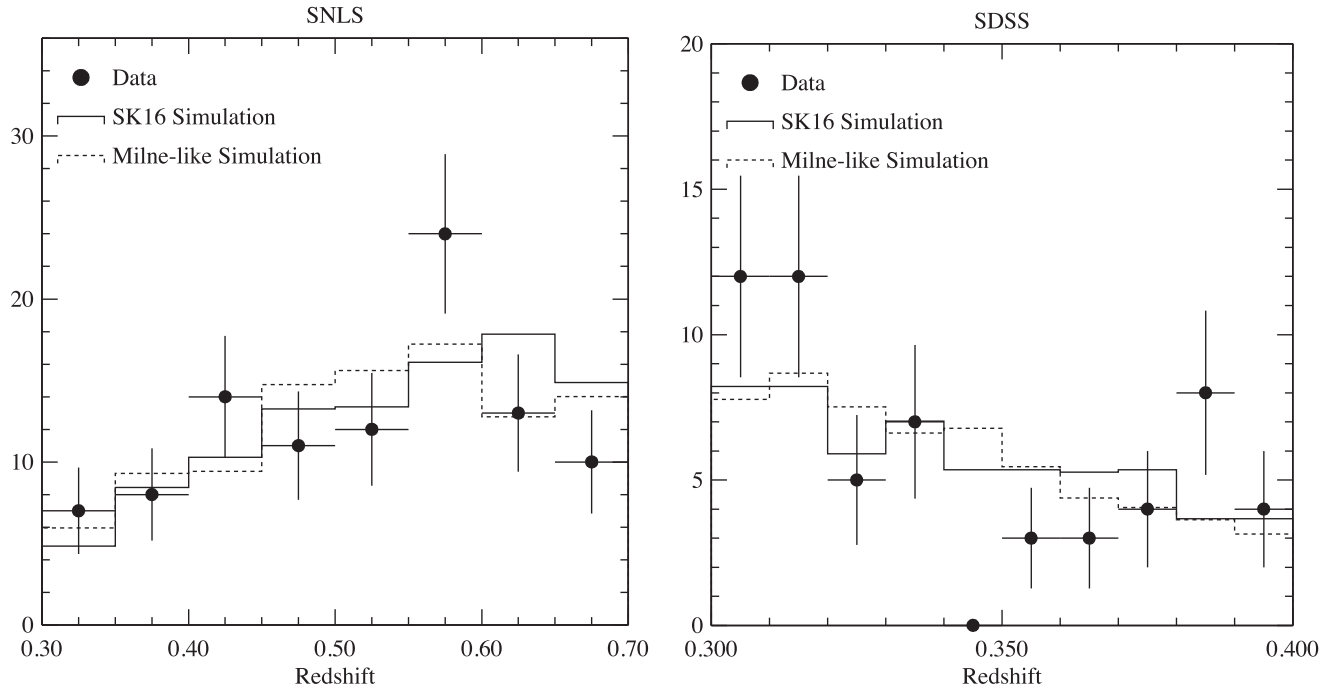


**Figure 5.** The redshift distribution of the SN Ia accepted in the analysis comparing the data and simulations of the SK16 and Milne-like models as described in the text in the SNLS (left-hand panel) and SDSS (right-hand panel) surveys.

broader distribution for the Milne-like model than the SK16 model. The distribution of the fitted value of $c$ is sensitive to the different predictions of the two models.

We note that the rest-frame colours are highly correlated with the fitted value of $c$ and considering only one of the distributions, $c$ or $u - v$ colour for example, is sufficient to discriminate between the SK16 and Milne-like models for the brightness of SNe Ia in the rest-frame ultraviolet.

## 4 COMPARISON OF SURVEY OBSERVATIONS AND SIMULATIONS

We apply the analysis described above to the data from the SDSS and SNLS supernova surveys in the JLA sample. This only includes light curves that have been clearly typed with spectroscopy as SN Ia, and thus their redshifts are well measured. Our analysis accepts 59 and 99 light curves in the SDSS and SNLS, respectively. After applying our redshift cuts to the JLA sample, the other cuts reject nine light curves ($5 \pm 2$ per cent), consistent with the simulation prediction or 9 per cent.

The redshift distributions for the SN Ia light curves accepted for analysis by both surveys agree well with the simulation showing that efficiency and selection effects are well modelled. The distributions for the SALT-II $x_1$ parameter and the uncertainty on the peak time also agree well between the simulation and the data showing that the results of the SALT-II fits to the accepted light curves are also well modelled by the simulation. The uncertainty on the peak time also contributes to the resolution of $B$-peak colours. The simulated results for both the SK16 model and Milne-like model in these parameters show no obvious dependence on the two underlying SN Ia light-curve models. Figs 5 and 6 compare the results of our simulations with the results of the data analysis for these parameters.

Fig. 7 compares the distribution of the fitted rest-frame colours among the SNLS and SDSS data with simulations of the SK16 and Milne-like models. Here the Milne-like model have 50 per cent red and 50 per cent blue light curves. The colours at $B$-peak clearly agree better with the SK16 model showing a wide distribution in $u - v$ rather than two narrow peaks in the SNLS as we would expect in the Milne-like model. For the SDSS, the $u - v$ distribution is slightly narrower compared to the Milne-like model. The comparison is less clear for the $u - b$ colour where the Milne-like model distribution is wider than the data, and the difference between the SK16 and Milne-like models is smaller. There is no obvious difference between the data and the two models in the $b - v$ colour.

Fig. 8 compares the distribution of the fitted SALT-II colour parameter between the data and the simulations. We considered three models of this distribution to compare with the data in a simple $\chi^2$ minimization. The first model is SK16, and it is fit to the data with fixed shape allowing only the distribution's area to vary. The second is the Milne-like model where the predictions for the fractions of blue and red light curves are taken from the observations displayed in fig. 4 of Milne et al. (2015); roughly 70 per cent and 30 per cent respectively in the SDSS corresponding to the redshift range of 0.3–0.4 and 80 per cent and 20 per cent in the SNLS in the redshift range 0.3–0.7. We also fit this model to the data only allowing its area to vary. The third is a variant of the Milne-like model where we allow the areas of the contributions from the red and blue distributions to vary independently.

In the SNLS data the SK16 model is decisively favoured. As can be seen on the right-hand panel of Fig. 8, this model, the solid histogram, agrees reasonably well with the data, dots, and gives $\chi^2 = 18$ for 8 degrees of freedom. Note that we did no tuning of the parameters of this model to match our data set, but simply used the parameters found in a very different analysis done by Scolnic & Kessler (2016). The Milne-like model with fixed fractions of blue and red light curves fits poorly, giving $\chi^2 = 49$. The Milne-like model with floating fractions of blue and red light curves also agrees poorly with the data giving $\chi^2 = 47$ for 7 degrees of freedom. This

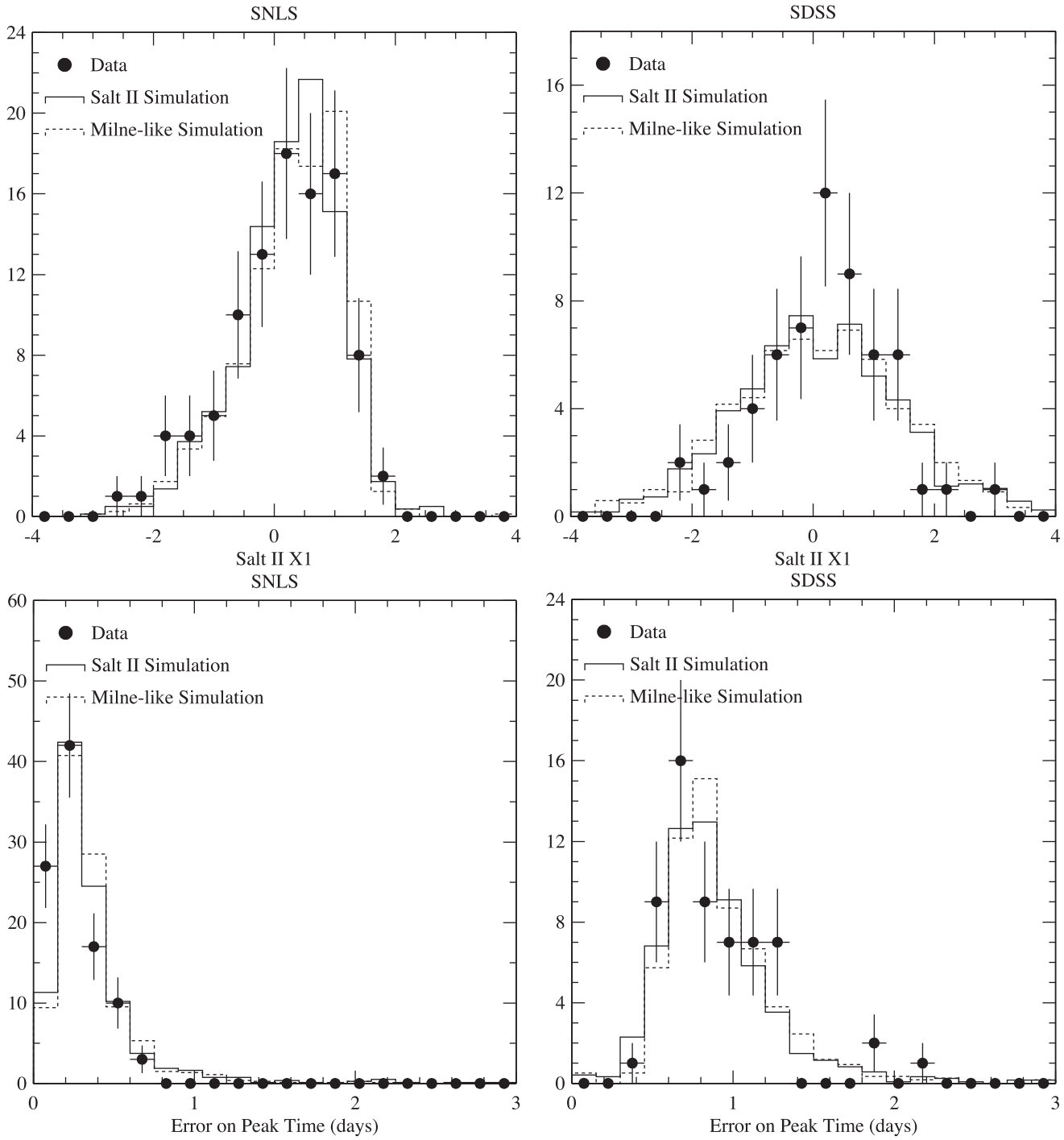


**Figure 6.** The distributions of the fitted values of the SALT-II $x_1$, stretch, parameter (top panels) and the uncertainty on the time of the *B*-peak (bottom panels) comparing the data and simulations of the SK16 and Milne-like models as described in the text in the SNLS (left-hand panels) and SDSS (right-hand panels) surveys.

fit has (41 ± 10) per cent of the light curves from the blue sample, and is displayed as the dashed histogram in the right-hand panel of Fig. 8. The relative probability of the Milne-like model based on the $\chi^2$ probability for these fits is smaller than $3 \times 10^{-6}$.

The results for the SDSS data, left side of Fig. 8, are not able to distinguish between the two models. The fit to the SK16 model agrees well, giving a $\chi^2 = 7$ for 9 degrees of freedom and is shown by the solid histogram. The fits to the Milne-like model with fixed blue and red light-curve fractions give $\chi^2 = 12$, and the Milne-like model with floating light-curve fractions gives $\chi^2 = 12$ for 8 degrees of freedom with (49 ± 16) per cent blue light curves. This latter fit is shown by the dashed histogram. That the SDSS data have poorer discrimination power than the SNLS data is not surprising given the smaller number of SN Ia in the SDSS sample and poorer resolution on the peak colours than the SNLS. Nevertheless, the SDSS data show excellent agreement with the SK16 model.

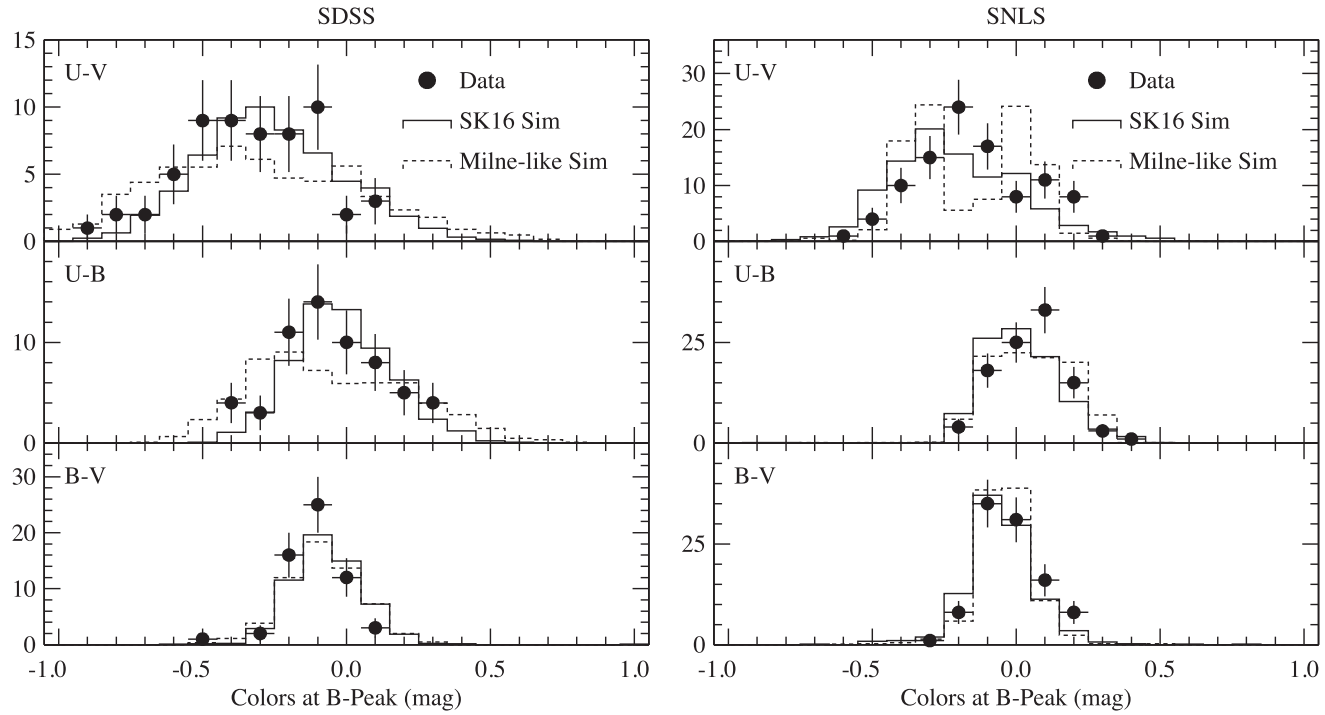


**Figure 7.** The fitted rest-frame *B*-peak colours comparing the data and simulations of the SK16 and Milne-like models in the SDSS (left-hand panel) and SNLS (right-hand panel) surveys.

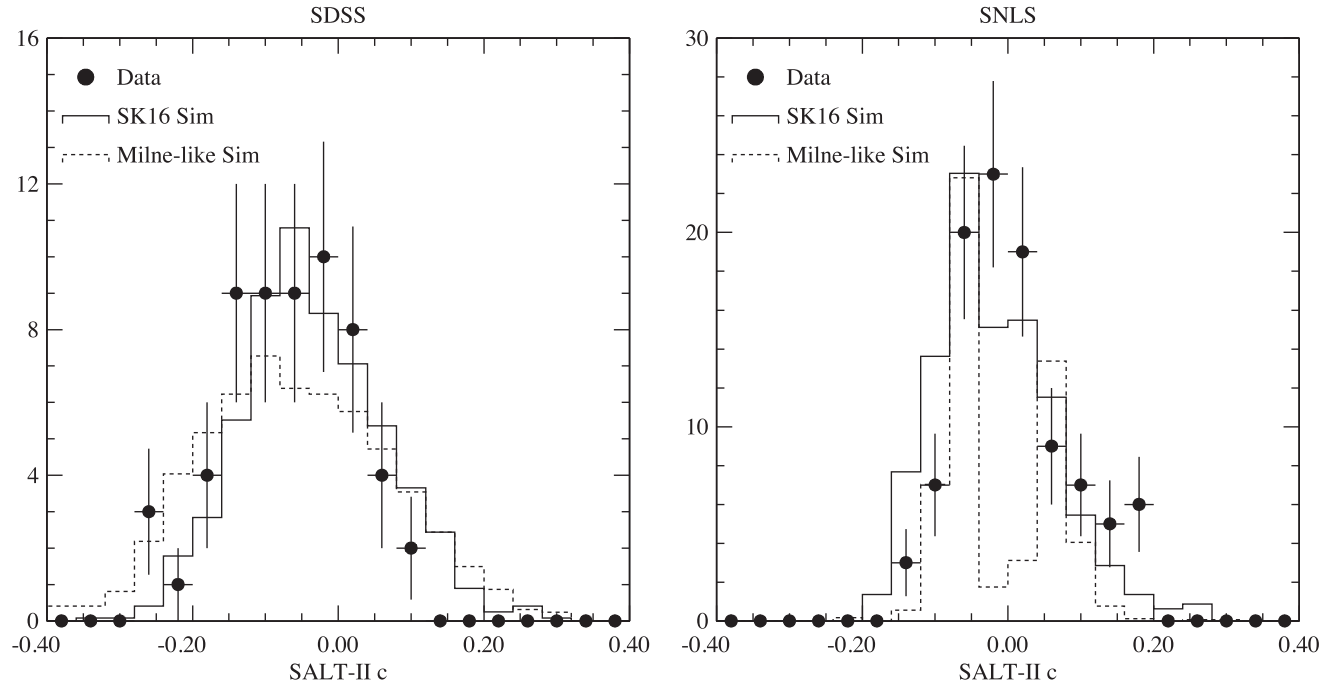


**Figure 8.** The fitted SALT-II colour parameter comparing the data and simulations of the SK16 and Milne-like models in the SDSS (left-hand panel) and SNLS (right-hand panel) surveys.

We explore variations of the Milne-like model consistent with the Milne et al. (2015) observation including details of the bifurcation in the ultraviolet and the size of the colour separation. We reduced the wavelength range of the bifurcation between the red and blue samples from 2700–4300 Å to 2700–3700 Å and varied the $u - v$ red and blue colour separation in the range of 0.26–0.55 mag from the central 0.46 mag. Those with a smaller colour separation agreed better with the SNLS data, but never having a $\chi^2$ probability relative to the SK16 model larger than $4 \times 10^{-5}$. Any SN Ia model that has two narrow features in the *B*-peak $u - v$ colour separated by more than 0.25 mag does not agree well with the data. Adding additional colour smearing to the Milne-like model would make it agree better with the data, but would be inconsistent with the narrow widths of the colour peaks seen in Milne et al. (2015).

## 5 CONCLUSIONS

Our analysis of the SDSS and SNLS supernova surveys does not agree with the observations reported in Milne et al. (2015). We do not observe two distinct red and blue samples in the rest-frame NUV brightness of SN Ia at *B*-peak. Rather, we see a broad distribution well described by a combination of SN Ia colour variations and extinction as given by the SALT-II model with a data-derived distribution of its parameters, the SK16 model. Our simulations of the two surveys show that we can distinguish between the two $u - v$ colour models, and our analysis of 158 light curves, specifically the 99 from the SNLS, show no evidence for the distinct $u - v$ peaks reported in Milne et al. (2015).

## ACKNOWLEDGEMENTS

We thank Peter Milne and Ryan Foley for useful discussions about their work. This work was supported in part by the Kavli Institute for Cosmological Physics at the University of Chicago through grant NSF PHY-1125897 and an endowment from the Kavli Foundation and its founder Fred Kavli. RK and DS gratefully acknowledge support from NASA grant 14-WPS14-0048. DS is supported by NASA through Hubble Fellowship grant HST-HF2-51383.001 awarded by the Space Telescope Science Institute, which is operated by the Association of Universities for Research in Astronomy, Inc., for NASA, under contract NAS 5-26555.

## REFERENCES

Astier P. et al., 2006, A&A, 447, 31
Betoule M. et al., 2014, A&A, 568, A22
Breeveld A. A., Landsman W., Holland S. T., Roming P., Kuina N. P. M., Pagea M. J., 2011, in McEnery J. E., Racusin J. L., Gehrels N., eds, AIP Conf. Proc. Vol. 1358, An Updated Ultraviolet Calibration for the Swift/UVOT. Am. Inst. Phys., New York, p. 373
Frieman J. A. et al., 2008, AJ, 135, 338
Guy J. et al., 2010, A&A, 523, A7
Kessler R. et al., 2009, PASP, 121, 1028
Kessler R. et al., 2013, ApJ, 764, 48
Milne P. A., Foley R. J., Brown P. J., Narayan G., 2015, ApJ, 803, 20
Olive K. A., Particle Data Group, 2014, Chin. Phys. C., 38, 090001
Perlmutter S. et al., 1999, ApJ, 517, 565
Riess A. G. et al., 1998, AJ, 116, 1009
Roming P. W. A. et al., 2005, Space Sci. Rev., 120, 95
Schlegel D. J., Finkbeiner D. P., Davis M., 1998, ApJ, 500, 525
Scolnic D., Kessler R., 2016, ApJ, 822, L35
Scolnic D. et al., 2014, ApJ, 795, 45

## APPENDIX:

The list of the SNe Ia used in this analysis.

The SNLS ID: 03D1au; 03D1aw; 03D1fc; 03D4au; 03D4cz; 03D4dh; 03D4dy; 03D4gf; 03D4gg; 04D1hd; 04D1hx; 04D1jg; 04D1kj; 04D1oh; 04D1pg; 04D1rh; 04D1sa; 04D2an; 04D2fp; 04D2fs; 04D2gb; 04D2gc; 04D2iu; 04D2mc; 04D2mh; 04D2mj; 04D3co; 04D3df; 04D3do; 04D3fk; 04D3kr; 04D3nh; 04D4an; 04D4bq; 04D4fx; 04D4gg; 04D4ib; 04D4ic; 04D4in; 04D4jr; 04D4ju; 05D1cc; 05D1ck; 05D1dn; 05D1dx; 05D1ee; 05D1hm; 05D1ix; 05D1ke; 05D1kl; 05D2ab; 05D2bv; 05D2cb; 05D2ci; 05D2ck; 05D2dt; 05D2dw; 05D2eb; 05D2hc; 05D2he; 05D2ie; 05D2le; 05D2mp; 05D3cf; 05D3ci; 05D3dd; 05D3gp; 05D3jq; 05D3jr; 05D3lb; 05D3lc; 05D3mh; 05D3mx; 05D4af; 05D4av; 05D4bf; 05D4bm; 05D4cw; 05D4dt; 05D4ef; 05D4ej; 05D4ek; 05D4ff; 05D4fo; 06D2bk; 06D2ca; 06D2cc; 06D2ck; 06D3cc; 06D3el; 06D3et; 06D2gb; 06D3df; 06D3ed; 06D3em; 06D4ba; 06D4bo; 06D4co; and 06D4cq.

The SDSS CID: 1166; 1688; 2533; 4241; 4679; 5183; 5391; 5737; 5844; 5966; 6100; 6137; 6649; 6699; 6924; 7143; 7475; 7779; 8598; 9045; 9207; 10550; 12883; 13136; 13830; 13934; 14397; 14456; 14735; 15170; 15213; 15217; 15383; 15456; 15704; 15756; 15776; 16000; 16093; 16211; 16232; 16421; 16779; 16789; 17528; 18091; 18617; 18782; 19029; 19033; 19632; 19818; 20106; 20142; 20184; 20186; 20245; 20432; and 21042.

This paper has been typeset from a TEX/LATEX file prepared by the author.